ELECTRICAL TREES IN SOLIDS

Insulators are materials across which a high voltage can be applied without causing an appreciable electric current to flow. However, when the electric field is higher than the electric strength, this ceases to be the case and the material becomes conducting. In these circumstances it is said to have suffered a dielectric breakdown. We are most familiar with this phenomenon through its occurrence in atmospheric gases during a thunderstorm, where it takes the visible form of lightning. A "stepped leader," originated by high electric fields in the storm cloud, moves toward the ground by stepwise ionization of the gases via the high field generated at its tips as it propagates. A conducting path is only established when a leading tip makes contact with the ground, at which time a "return stroke" carries the current between the ground and the cloud. The branched structure of the stepped leader then becomes visible as forked lightning. This form of electrical breakdown is thus a two-stage process with the branched stepped leader acting as a precursor to the main discharge event.

Dielectric breakdown in solids does not always follow this pattern. There are many possible mechanisms which may lead to breakdown (1). All of these can be characterized by an energy balance equation in which the amount by which the input power exceeds the power removed from the material alters factors such as the temperature and conductivity. The excess power can be used to modify the material and reduce its insulating capability. At low fields a balance can be established in which the input power and power removed are equal, and an equilibrium is achieved. However, above a field, termed the breakdown strength, an energy balance can no longer be maintained. In this case, changes to the material properties brought about by the absorbed electrical power increase the rate of absorption and thereby accelerate the material modifications until breakdown ensues. Minor local differences in material properties favoring the mechanism amplify the mechanism in their vicinity via its positive feedback aspect. This local reinforcement causes the conducting path to be concentrated into a narrow tube extending from electrode to electrode. An example of a mechanism like this is provided by the heating produced when a dielectric material passes a current. In insulators the conductivity increases when the temperature increases, and thus the passage of a current will increase the current density via the increase in temperature and hence accelerate the rate of rise in temperature.

A different electric strength is associated with each mechanism, and insulating systems should be designed so that the applied field during service is considerably smaller than the lowest of these fields. Safety coefficients are taken into account, for this purpose, which derive from the long-term expected performance of insulation and thus allow for aging. Solid insulating systems should therefore not break down when used to specification. However, evaluation of these design coefficients is not straightforward.

Both liquid and solid insulating systems may, moreover, contain local defects such as metal or semiconductive protrusions (asperities) and gas-filled voids. Such defects raise the electric field in their vicinity, so that the design stress can be locally exceeded. In the case of the voids, this occurs because their gaseous contents break down at applied fields lower than those required to break down the surrounding material. The breakdown is therefore confined to the void and is called a partial (or void) discharge. During its limited duration (~10 ns to 1 μs) the void acts like a conductor and raises the field in the surrounding material as does the metal or semiconductive asperity. Over a period of time, the high local fields initiate a breakdown pattern similar to that of lightning in both liquid and solid insulation even though the average applied electric field is below the breakdown field of the material. The branched prebreakdown structure that is formed is termed an electrical tree. In contrast to gases, however, electrical trees in liquids and solids require the production of gas-filled low-density regions rather than a path of ionized atoms and molecules (2,3). For this reason the time required for tree generation follows the order solids $\gg$ liquids $>$ gases. Another difference concerns the permanence of the tree. In gases, neutralization and convection restore the insulating properties. In liquids the interface with the low-density regions can be broken up, allowing the gases to escape from the region, thereby leading to some return of the insulating quality. However, in polymeric solids the damage is permanent and the insulating life of the material is terminated once the return stroke has occurred.

Electrical tree formation in solids is therefore studied with two major aims in view. One is to obtain a physical understanding of the mechanism so that more resistant materials can be developed, and the other is to identify measurable features which can be used to diagnose the presence of a tree and hence allow insulation replacement prior to breakdown.

PHYSICAL DESCRIPTION

General

Electrical trees in solids exhibit a variety of shapes ranging from the sparsely branched form of Fig. 1 to the compact bush (ball) form of Fig. 2. In all cases, they possess a microscopic structure composed of roughly cylindrical gas-filled tubules (4) connected together. The walls of the tubules (sometimes referred to as channels; see ELECTRICAL TREES, PHYSICAL MECHANISMS AND EXPERIMENTAL TECHNIQUES) do not conduct appreciably. Although the tree has a black appearance in photographs produced by transmitted light, this is due to differences between the refractive index of the polymer and the gas the tubules contain, and not carbonization. In some materials imaging by reflected light reveals white glasslike tree structures, and in other cases they may appear brown, perhaps because of condensed decomposition products. During propagation the tree extends in steps by the addition of new tubules of diameter ~1 μm and length between 4 μm and 10 μm.

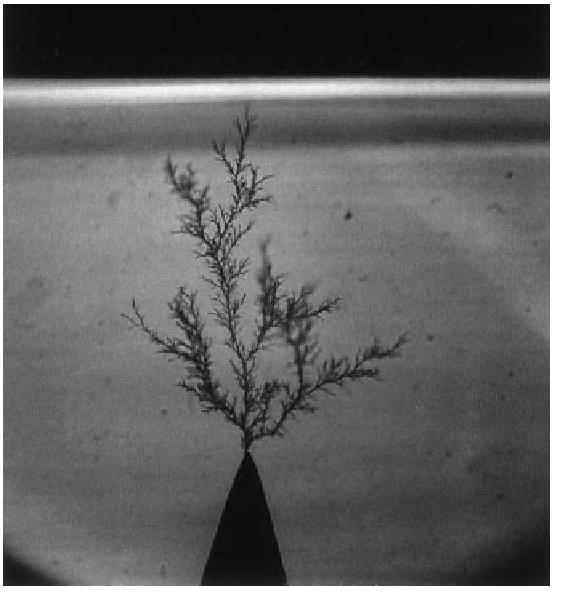

Figure 1. Branched form of electrical tree structure grown from a needle electrode (the black triangle is the needle tip, magnified ×34).

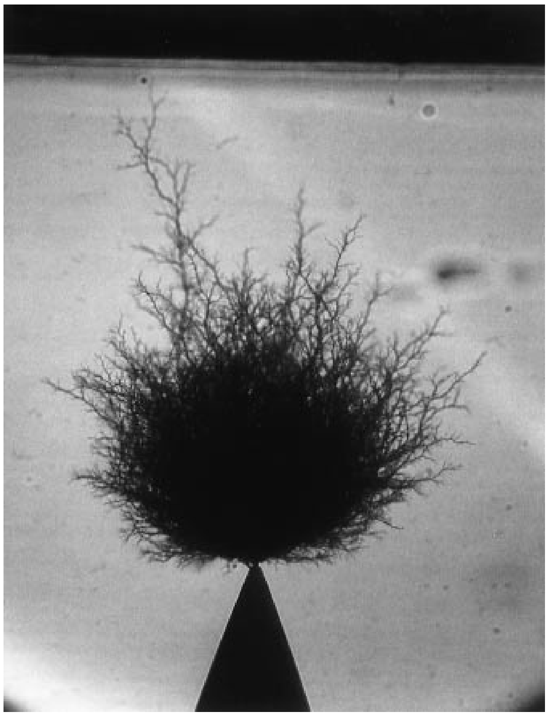

Figure 2. Bush form of electrical tree structure (the black triangle is the needle tip, magnified ×34). The trees of Figs. 1 and 2 are grown with needles of 3 μm tip radius in the same material, epoxy resin, under a 50 Hz ac voltage, with the tree of Fig. 1 formed at 8 kV, point-plane distance 1.53 mm, and that of Fig. 2 at 15 kV, point-plane distance 2.6 mm.

Repeated bifurcations occur, particularly in bush structures, and in this case the tubules often connect in the form of closed loops. As the tree propagates, the tubules first formed may widen and in some cases they can reach a diameter of ~50 μm.

Fractal

Electrical trees in solids have a statistical fractal (5) structure. In fractal structures a portion of the structure of size bL (with $b < 1$) will reproduce the complete structure, of which it is a part, when magnified up to the overall size L. This statement implies that if we measure the mass, M, or volume, V_{vol}, of the material from which the fractal is constructed, their relationship to the size L is given by

$$V_{\mathrm{vol}} \propto M \propto (L)^{d_t} \tag{1}$$

where d_t is the fractal dimension, so that the mass of the portion of size bL is given by

$$V_{\mathrm{vol}}(bL) \propto M(bL) \propto (bL)^{d_t} \propto (b)^{d_t}(L)^{d_t} \propto (b)^{d_t}M \tag{2}$$

A structure is a fractal when the dimension d_t is less than the Euclidean space in which the structure is constructed. Usually the fractal dimension d_t is not an integer. In the case of geometrical fractals, specific substructures of size b^n (with n an integer) can be identified, which, when magnified by the amount b^{-n}, exactly reproduce the overall structure. With electrical trees, however, this is not the case. Magnification does not reproduce the overall figure exactly. Instead, an average of all substructures of size bL contained within the tree yields a mass/volume which relates to that of the whole tree via Eq. (2). This holds for any value of bL lying between the minimum tubule length and the overall tree length. Structures like this are called statistical fractals. Measurement of the tree mass over a range of values of b and the use of Eq. (2) yields a value for the fractal dimension (d_t) of the tree (6). The effect of applying the magnification process to substructures within a branched tree is shown in Fig. 3.

The usefulness of determining the fractal dimension of electrical trees is twofold. Firstly, it replaces abstract descriptions of tree shape with a quantitative measure, and secondly it allows the volume/mass of polymer that has been converted to gas in forming the tree tubules (tree damage) to be related to the tree length, which is the feature of electrical trees that is most often measured. This latter factor has proved to be of great help in the development of physical theories for the treeing mechanism.

The fractal dimensions of branch trees are less than 2, and hence reasonable estimates of their value can be obtained by analyzing the photographic images which are projections of the tree onto a two-dimensional plane. Measured values of d_t for branch trees have been found to increase from 1.2 to 1.8 as the applied voltage was increased (7). Material morphology also has an effect upon the fractal dimension, as shown by its increase when measured in a polyester after different stages of curing (8). Other factors known to influence d_t are temperature (9), the presence of absorbed water [see (2) and (34)], and frequency (1). Increasing the applied voltage at room temperature causes the tree to change shape to a bush structure at a specific voltage level which reduces as the frequency of the applied field increases (10). The fractal dimension of bush trees is greater than 2, and sectioning (actual or optical) is required for their measurement. Values in the range 2.2 to 2.6 have been found (11). At very high voltages and frequencies, trees sometimes change shape as they propagate. In particular, branch structures may initiate at the periphery of a bush tree, producing what is called bush–branch structures. Though less useful here, the fractal concept can still be of help if d_t is given separate values for each part of the structure, since they will define the amount of damage required to advance that part to a given length.

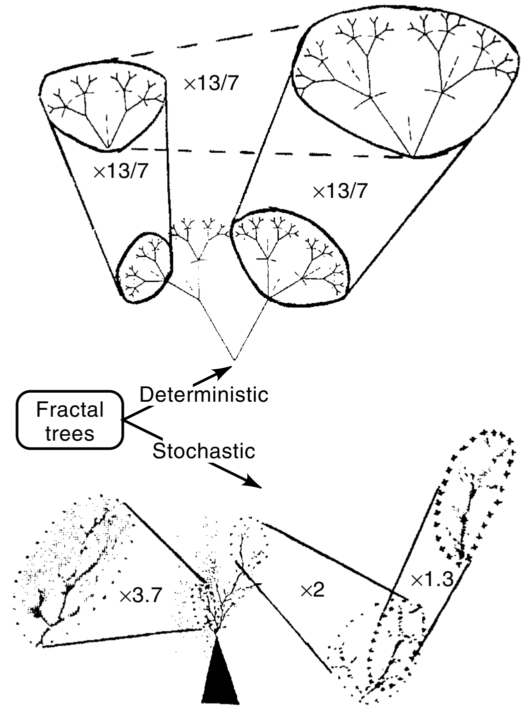

Figure 3. Illustration showing to what extent magnification of a portion of an electrical tree structure reproduces the original complete tree. Magnification of a tree-like geometrical fractal is given for comparison.

TREE GENERATION

Electrical tree generation is usually studied through laboratory experiments on samples containing either (a) an embedded needle electrode to which a high-voltage power supply is connected or (b) an artificial void of defined shape (12). Trees are produced only when the applied voltage exceeds a threshold level, whose value varies with the electrode geometry as well as the material and ambient conditions. Estimates of the applied field from the system geometry only yield the Laplace value and do not take into account any modification due to space charge. Trees are most easily generated by alternating current (ac) voltages, for which the Laplace value of the threshold field is low (e.g., ~150 MV/m). They can, however, be generated by direct current (dc) voltages applied to needle electrodes when (a) an impulse is applied, (b) the voltage is ramped up, (c) the electrode is short circuited, or (d) the polarity is reversed. In the dc case, the threshold Laplace fields required are higher (e.g., ≥ 500 MV/m) than for the ac case, with the highest values being associated with the lowest ramp rates. Insulation systems used in ac conditions (e.g., power transmission) and dc conditions (e.g., optical telecommunications) are thus both at risk of failure via electrical tree generation.

Dynamics

Initiation and Propagation. The generation of electrical trees in solids occurs in two distinct stages: initiation and propagation (growth). During initiation (i.e., time to inception), material modifications take place on the submicroscopic scale and are difficult to identify (see ELECTRICAL TREES, PHYSICAL MECHANISMS AND EXPERIMENTAL TECHNIQUES). Eventually, however, a gas-filled tubule or spheroidal void of ~10 μm size appears (inception) and tree propagation is initiated. The time required for initiation depends strongly upon the applied voltage and varies from as short as nanoseconds to times much longer than those needed for the tree to propagate across the insulation. This also can range between seconds and weeks depending upon the conditions. During propagation the tree advances in a stepwise manner by the addition of tubules to the existing tubular network (2). The fastest tree propagation, as measured by the dependence of their length upon time, occurs at the start of growth. Here it is even possible to resolve the addition of individual tubules. As the tree extends, its rate of propagation reduces (see Fig. 10 of ELECTRICAL TREES, PHYSICAL MECHANISMS AND EXPERIMENTAL TECHNIQUES). Sometimes a tree may even stop extending altogether, that is, it is said to passivate. This is more common in liquid insulators than in solids, and it is associated with trees whose fractal dimension is greater than 2 (i.e., bush trees). The mechanism of electrical tree propagation therefore has self-inhibitory tendencies in contrast to the accelerating behavior of breakdown at high uniform applied fields. During this phase of propagation, the time, t, dependence of the tree length is related to the fractal dimension via

$$(L)^{d_t} \propto V_{\mathrm{vol}} \propto t \tag{3}$$

This relationship shows that the tree propagation rate slows down as it becomes longer, because the volume of tree damage and hence the time required to increment the length by a given amount increases with the length. Consequently, if bush trees and branch trees are produced under the same conditions (particularly voltage and temperature), the bush tree propagation rate will be the slower one (2,10), since the bush trees contain the greater volume of damage within a given length.

Catastrophic Failure. As a tree becomes very long, its propagation rate starts to increase. This increase is associated with a rise of the rate at which damage is produced brought about by an increase in the field at the tree tips as the ground plane electrode is approached. Eventually, one (or at most a few) of the most advanced branches of the tree makes contact with the ground electrode. This establishes a path connecting the electrodes in which the insulating material is the gaseous contents of the tubules. Although the potential difference between the two ends of this path is sufficient to break down the gases in an open environment (~2 MV/m to 4 MV/m for air at atmospheric pressure), the narrow width of the tubules and the tortuous path often prevent this from happening immediately. Sometimes, several hours are required while the contacting tubule or tubules are widened. Eventually, one tubule is wide enough for gas breakdown to produce an arc connecting the electrodes by the shortest path through the tree. Polymeric materials melt at the high temperatures of the arc, giving rise to a wide (≥ 1 mm diameter) unbranched tube and a permanent short-circuit of the insulation.

Voltage and Frequency Dependence

Initiation. Tree inception at needle electrodes requires an applied voltage in excess of a threshold level. Estimates of its value are often made using a set of nominally identical needle electrode samples. Sometimes the applied voltage is ramped up, at a defined rate, until half of the samples have initiated trees (12). This voltage is defined as the 50% inception voltage, or $V_I(50)$. While this value is useful to make comparison between different materials and conditions (13), it is not a true measure of the minimum voltage required for inception, since the ramp experiments only allow a very short period of time for the completion of the initiation process at any given voltage level. A better estimate of the threshold value is obtained by maintaining the voltage level at a constant value and measuring the time required for half the sample set to initiate trees. In this way it is found that trees can initiate at voltages below that measured in the ramp experiment. However, the time to inception, t_I, asymptotically approaches infinity at a certain voltage level which could thus be taken to be the true threshold. Even this type of experiment is limited as to the time available (weeks to months), and it therefore makes no allowance for any long-term aging. The threshold voltage level obtained should thus be regarded as a property of the material system as prepared. Because t_I approaches infinity, empirical expressions for its voltage dependence relate to the voltage range investigated. Even outside of the threshold region, the voltage dependence is very strong. An expression available for this dependence which provides a good fit to the data (see Fig. 4) derives from a theoretical model (2,12)

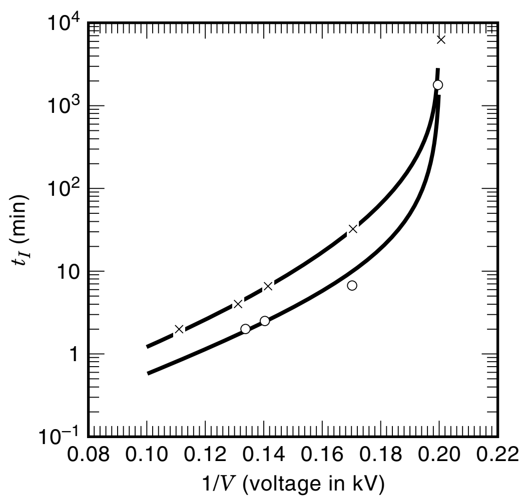

Figure 4. The voltage dependence of t_I (at 50% probability) from Eq. (4) given by the lines is compared to experimental data (×, steel electrodes; ○, silver electrodes). This plot shows that the voltage dependence of the time to initiation is strongly influenced by the presence of a voltage threshold. From Ref. 2.

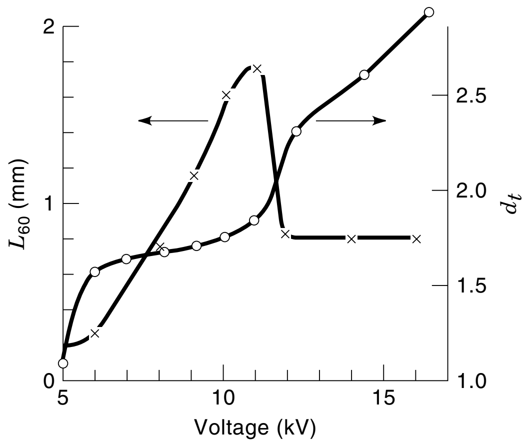

Figure 5. A comparison of the theoretical voltage dependence of L_{60} to experimental data for L_{60} (×) and the fractal dimension d_t (○).This plot shows the nonmonotonic growth rate that results when the fractal dimension increases with voltage. From Ref. 10.

that relates tree initiation damage to injection currents above a specific material threshold level. When the geometrical factors that relate the applied voltage V to the electric field at the initiating needle point are abstracted as a logarithmic contribution to the factor b, Eq. (4) results:

$$\log(t_I) = (a/V) + b - \log\{(1/V_t) - (I/V)\} \quad (4)$$

Here V_t is the threshold level (in volts), a is a constant depending upon the electrode material (specifically the 2/3 power of its work function), b is a constant depending upon the insulating and electrode materials (i.e., the ratio of energy factors for tree-forming damage and injection currents), and including logarithms of the frequency, and an electrode geometry factor. The reader is referred to Refs. (2) and (12) for details. The dependence upon ac frequency contained in Eq. (4) predicts an inverse frequency dependence for t_I. Although it is known that t_I reduces at high frequencies, insufficient data have been obtained as yet to verify the predicted dependence.

Propagation. The voltage dependence of propagation has been measured by comparing the tree length after a given propagation period, usually one hour (i.e., L_{60}), under different voltage levels and identical conditions of temperature and frequency. This measure exhibits an unusual feature in that it is nonmonotonic (see Fig. 5). As the voltage is increased above the threshold level, L_{60} first increases, then beyond a crossover voltage it decreases to a plateau region. L_{60} resumes an increasing trend at still higher voltages. The explanation for this behavior (10) lies in the changes in tree shape brought about by the voltage increase. The crossover voltage corresponds to a sharp change from branch trees ($d_t \leq 1.8$) to bush trees ($d_t \geq 2.2$). Even though the rate of damage production increases as the voltage increases, the extra amount of damage required to form bush trees of the same length as branch trees causes L_{60} to decrease. At higher voltages a change to a bush-branch shape occurs and the faster-growing branch component of the complete tree allows L_{60} to increase again. At the highest voltages used, a relatively unbranched filamentary damage structure is sometimes observed to accelerate across the sample, corresponding to a limiting high field deterministic breakdown mechanism (14). The branch-to-bush crossover voltage is a function of the ac frequency, and it decreases as the frequency is increased. Noto and Yoshimura (33) have suggested that this transition is the consequence of an increased gas pressure within the tree structure; however, there is only limited evidence to support their contention.

Temperature Dependence

During operation, the conductive core of power cables heats the insulation material in contact with it to temperatures of the order of at least 70°C and sometimes as high as 90°C. On the other hand, insulation materials for superconducting cables will be expected to withstand temperatures as low as 77 K. It is therefore useful to have some knowledge of the effect that different temperatures have on the electrical treeing mechanism (13).

Initiation. At all voltages, the initiation time in polymeric materials used in power cable insulation shows very little change as the temperature is increased above 25°C until it reaches T ≈ 70°C, at which it drops sharply, by an order of magnitude, to a lower value which remains effectively unchanged from 80°C up to the melting point. Therefore, excessive heating at cable cores may speed up tree inception at potential initiation sites. The values of V_I required for inception at $T = 77$ K are higher than those found at room temperature and indicate a greater difficulty in initiating trees in polymers when they are in a glassy state.

Propagation. At temperatures ≥ 80°C, electrical trees have the branch form ($d_t < 2$) for all applied voltages. Also, trees with the same fractal dimension propagate more rapidly at higher temperatures. Both effects cause electrical trees to cross an insulating sample in a shorter time at high temperatures and hence to be more threatening to its survival. At $T = 77$ K, trees initially tend to form a compact structure of ~20 μm length, but then propagate in a branch form with $d_t \approx 1.3$. The rate of growth is slow, but the low fractal dimension partially offsets this. Before they become very large (i.e., $L > 10^2$ to 5×10^2 μm) the polymer cracks and mechanical fracture ensues. Overall it appears that though electrical trees are difficult to initiate at $T = 77$ K, once initiated they are very damaging to the insulation integrity.

Material Factors

Electrical trees are usually observed in insulating polymeric solids. These materials have a wide variety of chemical and physical compositions (15,16) which affect the initiation and propagation of electrical trees (13) (for details see ELECTRICAL TREES, PHYSICAL MECHANISMS AND EXPERIMENTAL TECHNIQUES).

Polymer morphology also influences tree generation. Polymers used for power cable insulation are semicrystalline; that is, they have regions where segments of the polymer chain align with crystalline regularity in the form of plates (lamellae) interspersed with regions of chain disorder which are amorphous. An alignment of the lamellae so that the amorphous regions follow the field lines at an initiating site will tend to favor initiation (17), as do microcracks aligned in the same way. The influence of material factors upon tree propagation has not been studied to the same extent as their effect upon initiation. Such data as are available indicate that the tensile strength has little effect compared to its influence upon tree initiation (see ELECTRICAL TREES, PHYSICAL MECHANISMS AND EXPERIMENTAL TECHNIQUES).

OBSERVABLE FEATURES ACCOMPANYING TREE FORMATION

Laboratory investigations allow a number of features associated with the treeing mechanism to be measured. Their identification and quantification serve a twofold purpose: (a) they provide a framework in which to establish the nature of the mechanism, and (b) they yield measurable quantities which may be used to estimate the progress of this prebreakdown phenomena.

Initiation

Light emission, acoustic emission, and electrical discharges have been observed during the initiation stage of trees generated by ac voltages applied to a needle electrode (2). The light emission, which has not been observed under dc voltages, is modulated at twice the frequency of the applied ac voltage. It lies predominantly in the range of visible wavelengths. This form of emission is evidence for the injection of charge by the electrode. Some of the charge is trapped and retained near the electrode. In the succeeding half-cycle, charge of opposite polarity is injected, part of which recombines with the trapped charge, while the rest is itself trapped and repeats the process. The emission process is called electroluminescence (18) and the details of its generation are not yet fully understood (see ELECTRICAL TREES, PHYSICAL MECHANISMS AND EXPERIMENTAL TECHNIQUES). After a period of electroluminescence, electrical discharges are also observed. These discharges are only present in the positive half-cycle and have magnitudes that in polyethylenes start at ~40 fC and rise to 100 fC. They are caused by processes whereby electrons moving toward the positively charged electrode gain enough kinetic energy to ionize the polymer along their path, hence doubling the number of electrons. A measurable discharge current is produced when the process develops into a chain reaction of electron generation called an avalanche. The discharge magnitudes observed correspond to 2.5×10^5 to 6.24×10^5 electrons. At the onset of tree initiation, discharges of ~100 fC start to occur on both half-cycles. These are accompanied by burst acoustic emission and the formation of the initial tubule of the tree.

It is not clear yet what role the electroluminescence plays in creating the conditions for tubule formation (see ELECTRICAL TREES, PHYSICAL MECHANISMS AND EXPERIMENTAL TECHNIQUES). Optical emission of this type has been observed to occur for days in polyethylene without a tree initiating. However, once measurable electrical discharges occur, a tree always results. In some cases, the formation of strings of microvoids (~1 μm in size) has been observed at this point, and it has been speculated that damage on a scale of 1 nm to 100 nm is being generated. In contrast to polyethylene, it has been reported (19) that for epoxy resins, fine filamentary damage is produced and converts to a tree tubule without the advent of any electrical discharges above 50 fC. In this case, the electroluminescence activity becomes more erratic when the damage is being produced, with some periods giving large emission counts followed by others with very little. Thus, it appears that electroluminescence must be related to damage generation in these materials.

Propagation

The tree is said to have initiated when a tubule of 4 μm to 10 μm length is formed. At this stage, discharges are observed to occur on every half-cycle with an initial magnitude of ~100 fC (2,20). These discharges are due to breakdown of the gases in the tubule. A minimum potential difference between the tube ends is required to cause its gaseous contents to break down (the discharge inception voltage), and its value depends on the product of cavity size and gas pressure. The observed size of the initial tubule corresponds to a cavity for which such gaseous breakdown occurs for the lowest inception voltage at atmospheric pressure. It is therefore an optimum size for an initial portion of the tree. Gases break down in much lower fields than polymers (e.g., the field required in the initial tubule is ~30 MV/m), and thus the electrical discharge is confined to the tubule and is termed a partial discharge. These discharges are accompanied by visible and ultraviolet (UV) emission together with impulse acoustic emission, which are features typical of gas discharges. After a period of time the discharges on the negative half-cycle are extinguished, leaving those on the positive half-cycle unchanged. At this point the tree starts to extend by the formation of an additional branch or branches. Sometimes it is possible to observe light emission from the tubule tip; and on occasions when the tree bifurcates, this splits into two regions. Once the tree branch extension has been completed, discharging on both half-cycles resumes. Now the total discharge measured is about twice that for a single tubule—that is, ~200 fC. In the early stages of propagation, further extension of the tree increases the discharge magnitude by approximately 100 fC for each additional 10 μm tubule; that is, each tubule appears to contribute equally to the discharge magnitude. The discharge magnitude per half-cycle, as well as its associated acoustic emission, can increase to as much as 1 nC as the tree extends. Whether or not the magnitude continues to be related to the number of tubules (amount of tree damage) is difficult to verify because of uncertainties in the number and size of tubules. Individual discharges take place in ~10 ns (21) and can be difficult to resolve from one another when they occur in a triggered sequence as opposed to randomly generated throughout the tree at different parts of a half-cycle.

The tree discharges are associated with the formation of the local damage (2) required to further extend the tree, with large numbers of discharges occurring at times of rapid extension. This damage takes the form of polymer chain scission leading to gaseous decomposition products composed of CO_2, CO, H_2, acetylene, and low-molecular-weight chain fragments in polyethylene. In epoxy resins, acid gases such as oxides of nitrogen may also be produced. These decomposition products have been detected by means of light emission spectra and also through mass spectroscopy from which they were found to be produced in bursts, consistent with a production mechanism associated with the discharges. It is considered that some of the decomposition species are chemically reactive and both physical and chemical degradation widens the tubules to some extent (see ELECTRICAL TREES, PHYSICAL MECHANISMS AND EXPERIMENTAL TECHNIQUES). They may also modify the tubule surfaces—for example, through the formation of conducting patches—and reduce its ability to discharge, through the presence of electronegative gases which raise the inception voltage required for gas discharges.

At some stage in a tree growth (usually when it approaches the plane electrode), its propagation rate starts to increase. At this point, electrical discharge activity decreases dramatically. The light emission associated with tubule discharges ceases and the acoustic emission returns to a level and form typical of the earliest stages of propagation. Thus ironically, when the tree reaches the penultimate stage prior to failure, indications of its presence become minimal.

DISCHARGES AND TREE SHAPE

Discharge behavior during electrical tree propagation is strongly correlated with the tree shape produced. Differences in shape can be related to variations in the spatial location of the discharges, their magnitude, the number within a given period, the phase of the ac cycle they occur on, and the shape of individual discharge pulses.

Branch Trees

Individual pulses in branch trees are narrow (1 ns to 2 ns). Their magnitude rises from initial values of 100 fC up to ≤ 1 nC for long trees (≥ 1 mm). As the tree propagates (22), there is a background in which the number of discharges remains nearly constant at ~200 pulses per second (pps). These discharges, which do not extend to the tree tips, are accompanied by widening of existing tubules together with branching along their length. Interspersed with this are bursts of great activity. In polyethylene the widths of these pulses are slightly wider than those of the background discharges. Their repetition rate is also greater, and in epoxy resins it reaches ≥ 1000 pps. These discharges predominantly lie within some sections of the tree connecting the needle electrode to tree tips. They are associated with tree extension from the tips involved. At very long lengths, when the tree propagation starts to accelerate, the magnitude of the discharges drops by up to four orders of magnitude though the number of pulses is close to that observed during the earlier bursts. Now the discharges are concentrated at the tips which extend rapidly.

Bush Trees

The pulse widths for bush trees in polyethylene are larger than those for branch trees, possibly because of the overlap of independent pulses. Their rate of production can reach ~2000 pps, and their magnitudes can reach values of ≥ 1 nC. They are concentrated in the body of the bush where they are associated with the large amount of branching characteristic of bush trees. If the point-to-plane gap is high, a bush tree may almost cease to propagate and the discharges are then concentrated on the periphery of the tree, where fine damage may be generated. Bursts of activity, like those noticed in branch trees, will be observed if a new branch structure originates on the bush periphery.

DISCHARGE PATTERNS FOR DIAGNOSIS

The phase dependence of discharge magnitude and number in electrical trees is very different from those found for gas-filled cavities, and this has been exploited to produce a diagnosis system for the presence of electrical trees in insulating materials. The occurrence of partial discharges tends to be concentrated in two quadrants of an ac cycle, namely, the positive ongoing quadrant and the negative ongoing quadrant. The precise phase at which a discharge may occur will change from cycle to cycle; and if their number and magnitude at a particular phase is integrated over a large number of cycles, a phase distribution will be obtained with a peak in each of the two quadrants. These distributions are usually skewed. The charge magnitude versus phase distribution for electrical trees shows a negative skewness (i.e., the distribution rises more slowly than it decreases as the phase increases) for the peaks in both quadrants (23). In contrast, nontreeing cavity discharges show, in general, a positive skewness, and thus they can be distinguished from discharges in trees (24). Higher-order moments (e.g., kurtosis) can also be used.

Significant information is also provided by the distribution in partial-discharge–pulse–charge magnitudes, q, which can often be well described (especially for positive discharges) by the two-parameter Weibull distribution:

$$F(q; \alpha, \beta) = 1 - \exp[-(q/\alpha)^{\beta}] \quad (5)$$

where α and β are scale and shape parameters, respectively. While α is a measure of charge magnitude (corresponding to the charge height at probability 63.2%), and thus is directly associated with the tree dynamics, β depends on the dispersion of partial discharge magnitude in the set of recorded ac cycles. The value assumed by β is characteristic of the phenomenon causing partial discharges. In the case of electrical trees, β ranges between ~0.7 and ~1.8, depending on applied voltage, material, and tree length. It has been observed, in fact, that the value of β can be associated with the fractal dimension of the tree, decreasing as this dimension diminishes (25).

All these quantities can be used to set up patterns for material characterization and tree investigation, possibly in combination with an objective evaluation tool. For example, neural networks can be employed to yield a clearer indication of the presence of trees and distinguish them from other discharge processes that may be occurring in the material (26). An alternative approach (27,28) has been to characterize the discharge sequence because this contains more information than the probability distribution. Here factors relating to the correlation of discharge sequences are obtained. The observed differences in discharge patterns for branch and bush trees indicate that an approach such as this should not only be able to demonstrate the existence of electrical trees, but should also be able to distinguish their shape.

THEORETICAL MODELS OF TREE FORMATION

The electrical processes that drive the production of electrical trees have been experimentally established and can be used to formulate theoretical models for the two stages of inception and propagation. Details of the physics and chemistry of damage generation, particularly at the molecular level, remain, however, only partly resolved (see ELECTRICAL TREES, PHYSICAL MECHANISMS AND EXPERIMENTAL TECHNIQUES).

Initiation

This stage of tree generation is brought about by the behavior of charges injected into the polymer, either in the high local field at a metal point or by means of void discharges. During charge injection the highest current density in the polymer will occur at the injecting point. All electric currents dissipate energy in the form of heat which could cause damage to the polymer if it raises the local temperature high enough. Thus it can be assumed that if the current density is higher than a given threshold value, some of the dissipated energy is used to cause local damage to the polymer. The injected charge moves into the polymer, and it eventually becomes trapped around the injecting site. This reduces the actual local field in the polymer from the high value it had initially, and consequently the injection current will reduce and eventually cease unless the applied voltage continues to be raised as in dc ramp experiments. In the latter case, injection will be maintained continuously, thereby producing local damage until sufficient damage has been accumulated to initiate a tree. Because the trapped charges reduce the field at the injecting point, and hence the injection current for a given applied voltage, a higher voltage is required to reach initiation than would be the case if no trapped charges were formed. Thus high ramp rates under dc voltage, which do not allow enough time for the injected charge to penetrate the polymer and reduce the field, exhibit low values of V_I compared to those found for slow voltage ramps. Because injection and trapping depend upon charge, polarity, and material properties, polarity effects will be found; for example, negative charges are more easily injected into polyethylene and thus V_I is higher in negative than in positive dc polarity.

If the applied dc voltage is ramped up to a level below that required to initiate a tree at the given ramp rate and then kept constant, the injection current will equilibrate with the exceedingly small diffusion current and damage generation will cease at an amount less than that necessary to initiate a tree. In order to initiate electrical trees at a dc voltage of this magnitude, a sequence of dc pulses can be used, with sufficient time between them to allow the injected charge to dissipate. The damage produced by each pulse will be accumulated, and after a given number of pulses a tree will be initiated. It is customary to define the electrical tree resistance of dc cables through the number of pulses to tree initiation at a given voltage level (12). By assuming that only currents above a given threshold caused damage and that this has to accumulate to a material dependent level for tree initiation, Eq. (4) for t_I was derived by relating the number of pulses to time via their repetition rate. However, a crucial assumption has been made. The currents take place in the presence of injected space charge, and Eq. (4) can only be obtained if it is assumed that the space-charge field is proportional to the local applied field prior to injection.

Equation (4) has also been taken to apply to tree initiation in ac fields where each cycle has been regarded as a pulse. In this case, experiment has shown that tree initiating damage is associated with avalanching extraction currents rather than injection currents. Nevertheless, the same form of expression results because the dependence of the current density upon the local electric field has approximately the same functional form in both cases when the local field is very high; that is,

$$J_{\text{av}} \propto \exp(-A/E_{\text{av}}) \qquad \text{and} \qquad J_{\text{inj}} \propto \exp(-A/E) \tag{6}$$

where J_{av} is the avalanche current density, J_{inj} is the injection current density, and A is a mechanism-dependent constant. In the case of injection currents, A is dependent upon both the electrode material and the polymer; but in the case of avalanches, it depends only on the pathlength of the avalanche and material factors. For J_{inj} E is the local field at the injecting point, but for avalanche extraction, it is more correct to refer J_{av} to the energy that would be gained by an electron over the avalanche path to the needle if no impact ionizations occurred. E_{av} is the average field over this path and is determined by the potential difference through which the electrons are accelerated. If the avalanche starts at a point of low potential in the polymer, as a result of the space-charge modification, $E_{\text{av}} \propto V$ as required for Eq. (4). It is therefore difficult to determine whether injection or extraction is responsible for damage generation in cases other than trees generated by ramped dc voltages. A rigorous investigation of the material dependence of the constants in Eq. (4), which may shed some light on the question, has not yet been carried out.

While it has been assumed that injection currents generate damage by local heating, there are many possible mechanisms whereby avalanche currents may act. Although local heating may occur, the impact ionizations produce trapped positive charges and very high, very local fields which may cause mechanical damage by electromechanical forces. Visible and possibly UV emission (29) may occur, leading to chemical degradation. All these possibilities have been suggested (2), but as yet none have been fully substantiated. The details of the molecular mechanisms involved in the initiation stage of electrical trees are thus still unresolved (see ELECTRICAL TREES, PHYSICAL MECHANISMS AND EXPERIMENTAL TECHNIQUES).

Propagation

During propagation, discharges in the tree tubules inject electrons into the polymer surrounding the tree tips and simultaneously raise the local field in the polymer. The conditions therefore exist for the generation of local avalanches in the polymer, which may cause damage via any of the mechanisms that have been suggested to operate during inception. The shorter time required for propagation as compared to inception would then be a consequence of both (a) the greater ease of charge injection from the tubule discharges as compared to metal points and (b) the larger kinetic energy associated with charge carriers in the discharge due to the longer mean-free path provided by the gaseous contents of the tubules. In addition, it has been suggested that the mechanical shockwave from the discharge could cause mechanical fracture. This is unlikely in elastomeric materials, because its magnitude contains only 0.002% of the discharge energy and is well below the level required to cause yielding—for example, in polyethylene (2). The discharge produces both heat and charged particles with a high kinetic energy (~10 eV), which may damage the polymer by ballistic impact with the tube walls. It has therefore been suggested that these processes, together with chemical degradation brought about by the visible and UV emission produced in the discharge, could "drill" a new tubule and extend the tree into the polymer. As with inception, in-

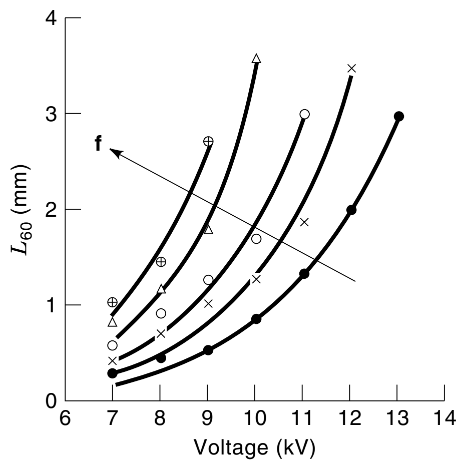

Figure 6. A comparison of the theoretical voltage dependence of L_{60} to experimental data obtained for branched trees with the same fractal dimension, $d_t \approx 1.7$, but grown at different frequencies. These trees were grown from a needle-shaped electrode obtained by recession of a needle electrode, in contrast to the data of Fig. 5, which were obtained for a fully embedded needle electrode. This plot shows the strong voltage dependence of the growth rate when changes in fractal dimension are removed from consideration. From Ref. 10.

sufficient data about tubule extension has been obtained to allow a choice to be made between the possible processes. An analytical expression relating the damage required for tubule extension to that produced by local avalanches restricted to a 10 μm distance from their point of initiation has been successful in reproducing the dependence of L_{60} upon voltage (10) (see Figs. 5 and 6). However, it is possible that a different mechanism of damage may give approximately the same functional dependence upon the local field, and hence reproduce the data just as well. Certainly the erosion processes will play a role in widening the tubules during discharging, a factor that was not allowed for in the theory. Other models for tree propagation are discussed in Refs. 30 and 31, with the latter associating propagation time to tree length and partial discharge activity.

The major questions that have to be answered regarding the propagation process are (a) why the tree grows as a tree and (b) what determines its shape. The key feature is the stepwise growth of the tree; however, the material morphology, by providing directions in which the tree can progress more easily, may also play a role. Stepwise growth allows succeeding extensions to take different directions from that of the original tubule if the conditions are favorable and hence lead to branch formation. A number of features may be responsible for a stepwise advance. Most important is the limited duration of the discharge. This takes place in ~10 ns, which is a tiny fraction of a half-cycle (typically 10 ms). The damage processes generated by each individual discharge are therefore restricted in duration. In particular, the increase in local field at the tube-tip is limited to a time ~10 ns. As a result, any avalanche generated by the high field will only experience the field for a short time and thus will be limited as to the range over which the electrons can gain enough energy to cause impact ionizations. Avalanches may also be restricted in range if the field in which they take place reduces along its path such as might occur if the accelerating field of the discharge is divergent. The positive ions produced by the impact ionizations also give rise to a decelerating field which may restrict the range of the avalanche unless it takes a self-sustaining filamentary form.

Stepwise growth allows for subsequent extension to be controlled by factors which render one or more directions favorable. Currently two different approaches have been proposed. In one case the choice of direction is stochastic; that is, it is made on the basis of probabilistic factors (32). The choice of direction is weighted so that directions along which the local field is greatest are the most likely to give an extension. The tree therefore extends in a particular direction as result of a field-dependent process, but random unknowable factors play a role. For example, random factors may determine which part of the tree suffers a tube discharge, leaving the rest unaffected, but the extension will then take place along the direction with the largest field. This approach yields structures with the fractal form observed experimentally. However, it is difficult to relate to a physical mechanism; and therefore it does not take factors such as material morphology into account in a realistic way, nor does it allow for damage to accumulate. Damage either extends to a new tubule or does not occur in this approach. The alternative approach is built on the accumulation of damage via limited range avalanches in the polymer. The damage generated is a function of the local field along each direction. It is assumed that the deposition and rearrangement of space charge during the discharges and avalanches causes the local fields to fluctuate about a near constant average value (10,22); that is, the local field exhibits deterministic chaos. Tubule extension occurs at the places where the damage accumulates first to a critical quantity. Linear extension is produced when the local field is determined by the discharge acting as a conductor, and branch formation occurs when the space charge at the tubule tip dominates. This approach generates structures which range from a nearly unbranched runaway to fractal branched and bush forms, depending upon the conditions placed on the accumulation of space charges and hence the fluctuation of the local fields. This physically based model has shown that material inhomogeneity only influences the tree structure through its effect on local fields. Figure 7 compares some structures obtained in the two approaches.

FUTURE DEVELOPMENTS AND UNRESOLVED QUESTIONS

Current research is concentrated on measuring the discharges and their pattern of occurrence during electrical tree propagation. Theoretical models are also being developed with the aim of simulating both the observed discharge behavior and its associated tree growth from basic mechanistic concepts. The recognition that discharges in tree propagation exhibit features of deterministic chaos (22) may prove fundamental in achieving this aim. At present, very little work is being carried out on the induction–initiation process. This can be expected to change as propagation becomes better understood and the models become more established. Attention is then likely to turn to identifying the tree at its onset by making use of the knowledge of the damage generating processes obtained from the study of propagation. There is also a need for a better understanding of the damage processes at a molecular level. Their study requires techniques with spa-

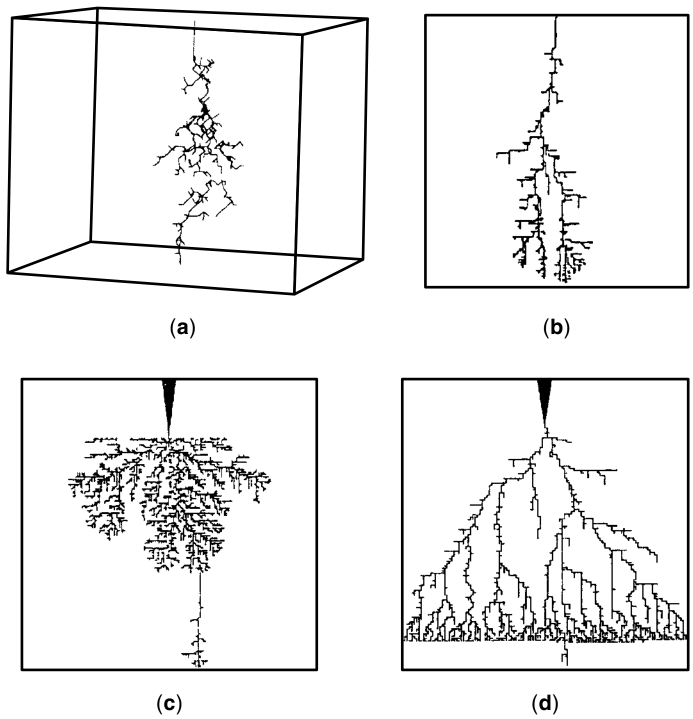

Figure 7. A tree structure produced by the stochastic model (a) is compared with a range of structures given by the physical model when different forms of local field fluctuation are considered. (b) Local fields proportional to the applied voltage. (c) Local fields capped at a fixed maximum level. (d) The capping value of the local field passes through a peak as the applied voltage is increased. Figure 7(a) taken from Ref. 6; Figs. 7(b–d) from Ref. 22.

tial resolutions down to ~1 nm to ~100 nm. Currently this area is not being investigated. The final unresolved question concerns the onset of accelerating tree growth. Other than a possible relationship to field enhancement as the plane electrode is approached, nothing is known about the conditions required. Further developments of the theoretical models may, however, provide some insight.

BIBLIOGRAPHY

1. L. A. Dissado and J. C. Fothergill, *Electrical Degradation and Breakdown in Polymers,* IEE Material and Devices Series 9, London: Peregrinus, 1992, part 3.
2. L. A. Dissado and J. C. Fothergill, *Electrical Degradation and Breakdown in Polymers,* IEE Material and Devices Series 9, London: Peregrinus, 1992, chap. 5.
3. G. Fitzpatrick, P. J. McKenny, and E. O. Forster, The effect of pressure on streamer inception and propagation in liquid hydrocarbons, *IEEE Trans. Electr. Insul.,* **25**: 672–682, 1990.
4. R. J. Densley, An investigation into the growth of electrical trees in XLPE Cable insulation, *IEEE Trans. Electr. Insul.,* **14**: 148–158, 1979.
5. B. B. Mandelbrot, *The Fractual Geometry of Nature,* New York: Freeman, 1977.
6. A. L. Barclay et al., Stochastic modelling of electrical treeing: Fractal and statistical characteristics, *J. Phys D, Appl. Phys.,* **23**: 1536–1545, 1990.
7. M. Fujii et al., Fractal character of dc trees in polymethylmethacrylate, *IEEE Trans. Electr. Insul.,* **26**: 1159–1162, 1991.
8. J. M. Cooper and G. C. Stevens, The influence of physical properties on electrical treeing in a cross-linked synthetic resin, *J. Phys. D, Appl. Phys.,* **23**: 1528–1535, 1990.
9. M. Ieda, Dielectric breakdown processes of polymers, *IEEE Trans. Electr. Insul.,* **15**: 206–224, 1986.
10. J. C. Fothergill, L. A. Dissado, and P. J. J. Sweeney, A discharge-avalanche theory for the propagation of electrical trees. A physical basis for their voltage dependence. *IEEE Trans. Dielectr. Electr. Insul.,* **1**: 474–486, 1994.
11. S. Kobayashi et al., Fractal analysis of 3d reconstructed patterns of real electric tree, *Conf. Proc. 5th ICSD,* IEEE Publ. 95CH3476-9, 1995, pp. 299–303.
12. T. Tanaka and A. Greenwood, *Advanced Power Cable Technology,* Vol. 1: *Basic Concepts and Testing,* Boca Raton, FL: CRC Press, 1983.
13. L. A. Dissado and J. C. Fothergill, *Electrical Degradation and Breakdown in Polymers,* IEE Material and Devices Series 9, London: Peregrinus, 1992, Chap. 7.
14. S. J. Dodd et al., Evidence for deterministic chaos as the origin of electrical tree structures in polymeric insulation, *Phys. Rev. B,* **52**: 16985–16988, 1995.
15. N. J. Mills, *Plastics: Microstructures, Properties and Applications,* London: E. Arnold, 1986.
16. C. Hall, *Polymer Materials: An Introduction for Technologists and Scientists,* London: Macmillan, 1981.
17. N. Hozumi et al., The influence of morphology on electrical tree initiation in polyethylene under ac and impulse voltages, *IEEE Trans. Electr. Insul.,* **25**: 707–714, 1990.
18. J. Jonsson et al., Spectral features of the luminescence of polyethylene subject to various excitation sources, *IEEE Trans. Dielectr. Electr. Insul.,* **3**: 859–865, 1996.
19. J. V. Champion, S. J. Dodd, and G. C. Stevens, Quantitative measurement of light emission during the early stages of electrical breakdown in epoxy and unsaturated polyester resins, *J. Phys. D, Appl. Phys.,* **26**: 819–828, 1993.
20. N. Hozumi, T. Okamoto, and H. Fukugawa, Simultaneous measurement of microscopic image and discharge pulse at the moment of electrical tree initiation, *Jpn. J. Appl. Phys.,* **27**: 1230–1233, 1988.
21. J. He et al., Partial discharge characteristics of electrical trees in polymeric cable insulation, *Ann. Rep. CEIDP,* IEEE 94CH3456-1, USA, Arlington, October 1994, pp. 91–96.
22. L. A. Dissado et al., Propagation of electrical tree structures in solid polymeric insulation, *IEEE Trans. Dielectr. Electr. Insul.,* **3**: 259–279,1997.
23. R. Bozzo et al., Stochastic procedures for the investigation of tree growth in insulating materials for HV applications. *Conf. Rec. IEEE I.S.E.I.,* IEEE 94CH3445-4, Pittsburgh, June 1994, pp. 269–272.
24. B. Fruth and L. Niemeyer, The importance of statistical characteristics of partial discharge data, *IEEE Trans. Electr. Insul.,* **27**: 60–69, 1992.
25. R. Bozzo et al., Inference of partial discharge phenomena in electrical insulation by charge-height probability distributions, Part 2: Extraction of partial discharge features in electrical treeing, *IEEE Trans. Dielectr. Electr. Insul.,* **5**: 118–124, 1998.
26. E. Gulski and A. Krivda, Neural networks as a tool for recognition of PD, *IEEE Trans. Electr. Insul.,* **28**: 984–1001, 1993.
27. T. Okamoto and T. Tanaka, Auto-correlation function of PD pulses under electrical treeing degradation, *IEEE Trans. Dielectr. Electr. Insul.,* **2**: 857–865, 1995.
28. M. Hoof, B. Freisleben, and R. Patsch, PD source identification with novel discharge parameters using counterpropagation neural networks, *IEEE Trans. Dielectr. Electr. Insul.,* **4**: 17–32, 1997.

29. S. S. Bamji, A. T. Bulinski, and R. J. Densley, Degradation mechanism at XLPE/Semicon interface subjected to high electrical stress, *IEEE Trans. Electr. Insul.,* **26**: 278–284, 1991.
30. G. Bahder et al., Physical model of electric aging and breakdown of extruded polymeric insulated power cables, *IEEE Trans. Power Appar. Syst.,* **101**: 1379–1390, 1982.
31. G. C. Montanari, Aging and life models for insulation systems based on PD detection. *IEEE Trans. Dielectr. Electr. Insul.,* **2**: 667–675, 1995.
32. L. Pietronero and H. J. Wiesmann, From physical dielectrical breakdown to the stochastic fractal model, *Z. Phys. B.,* **70**: 87–93, 1988.
33. F. Noto and N. Yoshimura, Voltage and frequency dependence of tree growth in polyethylene, *Ann. Rep. CEIDP,* 207–217, 1974.
34. J. V. Champion and S. J. Dodd, The effect of adsorbed water on electrical treeing in epoxy resins, *7th Int. Conf. Dielectric Materials Measurements Appl.,* IEE Conf. Pub **430**, 1996, pp. 206–210

L. A. Dissado
University of Leicester
G. C. Mazzanti
G. C. Montanari
University of Bologna